



HAL
open science

Estimation of carbon-dioxide production during cycling by using a set-membership observer

Nadia Rosero, John Jairo Martinez Molina, Maxime Chorin, Samuel Vergès

► **To cite this version:**

Nadia Rosero, John Jairo Martinez Molina, Maxime Chorin, Samuel Vergès. Estimation of carbon-dioxide production during cycling by using a set-membership observer. ECC 2021 - 20th European Control Conference, Jun 2021, Rotterdam (on line), Netherlands. pp.2323-2328, 10.23919/ECC54610.2021.9655078 . hal-03466931

HAL Id: hal-03466931

<https://hal.science/hal-03466931>

Submitted on 6 Dec 2021

HAL is a multi-disciplinary open access archive for the deposit and dissemination of scientific research documents, whether they are published or not. The documents may come from teaching and research institutions in France or abroad, or from public or private research centers.

L'archive ouverte pluridisciplinaire **HAL**, est destinée au dépôt et à la diffusion de documents scientifiques de niveau recherche, publiés ou non, émanant des établissements d'enseignement et de recherche français ou étrangers, des laboratoires publics ou privés.

Estimation of carbon-dioxide production during cycling by using a set-membership observer

Nadia Rosero^{1,2}, John J. Martinez², Maxime Chorin^{2,3} and Samuel Vergès³

Abstract—This paper presents a set-membership observer for the estimation of carbon dioxide production during cycling. The observer uses measurements of oxygen consumption and power at pedal level together with a discrete-time linear model of gas exchange dynamics. The real process is assumed to be disturbed by unknown but bounded disturbances. The proposed observer provides a deterministic interval which contains the real state. Since the excess of carbon dioxide production is linked to the overtake of the anaerobic threshold, the observer can be applied to predict the physiological state of the cyclist by using a reduced number of gas exchange sensors. The methodology is illustrated and validated using experimental data.

I. INTRODUCTION

Riding a bike is a worldwide usual activity not only as a sport, but also as a mean of transportation. During cycling, the human and the bicycle can be considered as a whole system composed by two main subsystems, which is susceptible to be improved in many ways. The first step for enhancing this system is to be able to measure and to understand the dynamical relationship between the variables of each part, in this case the link between physiological and mechanical variables.

Nowadays, connected objects and commercial sensors make it possible to monitor the cyclist-bike system. However, what happens within the body of the cyclist, in particular the dynamics of fatigue is difficult to assess, because of the need of either invasive or complex measurement systems (using blood sampling, or spirometric masks). Therefore, the fatigue dynamics is a subject of study of many physiologists, trainers and recently engineers, who analyze the relationship between measured variables and physiological markers of fatigue to develop medical and commercial products.

Since the works of [1] and [2] the gas exchange measures have been widely accepted for the determination of metabolic pathways (aerobic or anaerobic) used during physical activity. Also the identification of the anaerobic threshold, which is the point from which the production of mechanical power becomes less efficient, can be identified from gas exchange. Having a dynamical model of gas exchange during cycling constitutes an advantage in the study of physiological

behavior and to develop futures tools for improving the cyclist-bike system, for example for its use in control design.

Control techniques to regulate physiological variables while cycling have been recently implemented, among them the most popular is the control of Heart Rate (HR), thanks to its ease of measurements. For example [3], [4], [5] present techniques for controlling HR and the results show the difficulties to achieve an accurate control solution. On the other hand, the gas exchange variables are more strongly related to physical activity, although they are slightly harder to measure. In this regard, the work [6] presents a gas exchange model during cycling identified and validated using experimental data.

The implementation of control laws often requires the availability of the system states to make decisions, and a proper estimation of those reduces the need for sensors. In this aspect, observers are a useful tool, but the associated uncertainties of the estimation is often not quantified. In [7], [8] it is presented a set-membership observer (SMO) which provides both state estimations and their corresponding estimation error bounds. To study gas exchange, this kind of observer is interesting because of the biological nature of the considered system, whose parameters cannot be known with absolute precision and potentially vary over time. In addition, automated gas exchange analyzers are known to provide an estimation of gas exchange with limited accuracy [9], [10], [11], [12]. The SMO proposed in [7], [8] takes these phenomena into account under the form of bounded state and output disturbances, whose bounds are used in the design process to produce deterministic estimation error bounds. Estimation error bounds are useful in critical setups, such as supervised training, where the physiological limitations are strictly respected in order to guarantee the safety and the quality of training of the individual.

The main objective of this paper is to implement the SMO for the estimation of carbon dioxide (CO_2) production during cycling by using measures of oxygen (O_2) consumption and power at pedal level.

Firstly, the architecture of the observer is described in Section II. Secondly, the model of gas exchange dynamics while cycling is explained in Section III. Section IV explains the design of the SMO and its implementation in the cyclist-bike system. Finally, simulation results together with measured data from tests in cyclo-ergometer are presented to illustrate the contribution of the approach.

¹Nadia Rosero is with Departamento de Electrónica, Universidad de Nariño, Pasto, Colombia. nprosero@udenar.edu.co

²Nadia Rosero, John J. Martinez and Maxime Chorin are with Univ. Grenoble Alpes, CNRS, Grenoble INP, GIPSA-lab, 38000 Grenoble, France. john-jairo.martinez-molina@grenoble-inp.fr, maxime.chorin@grenoble-inp.fr

³Maxime Chorin and Samuel Vergès are with Univ. Grenoble Alpes, Inserm, CHU Grenoble Alpes, HP2, 38000 Grenoble, France. SVerges@chu-grenoble.fr

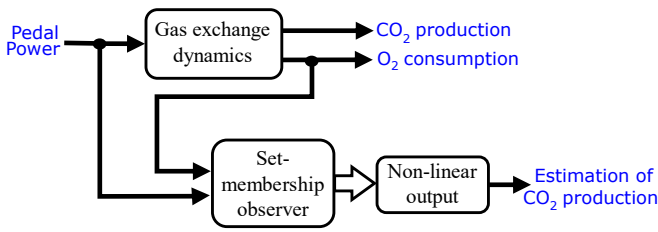


Fig. 1. Gas exchange dynamics and a set-membership observer architecture for CO_2 production estimation.

II. ARCHITECTURE FOR THE ESTIMATION OF CARBON DIOXIDE PRODUCTION

An architecture for the estimation of carbon dioxide production during cycling is proposed in this paper. This approach can be applied to quantify the current physiological state of the cyclist which is directly linked to the excess in carbon dioxide production.

The scheme for the implementation of the observer is depicted in Fig. 1. The complete cyclist-bike dynamics acts like a system of energy transformation where the power at pedal level can be seen as an image of internal chemical reactions involving oxygen consumption and carbon dioxide production.

The real system represented by the the block “Gas exchange dynamics”, has a power input and two outputs, which can be all measured in practice, but here we assume available measurements of the input and the oxygen consumption. A validated model of gas exchange dynamics (see [6]), is used for the implementation of the observer.

The state estimation is performed by using a SMO, which takes as inputs the power and oxygen consumption measurements and gives an estimation of the gas exchange variables. A non-linear output matrix, which depends on the estimated states is used to provide the estimation of the carbon dioxide production.

The components of the proposed architecture are discussed in more detail in the next sections.

III. MODEL OF GAS EXCHANGE DURING CYCLING

The gas exchange measurements during a physical activity are widely used by physiologists and trainers to assess the physiological state of an individual. Sensors used for oxygen consumption and carbon dioxide production measurements do not require invasive methods such as blood or muscle measurements and provide relevant information about chemical reactions in the body.

To perform an exercise, the synthesis of Adenosine Triphosphate (ATP), which is the energy source at cellular level, is required. It can be distinguished several pathways to obtain ATP, here, we will focus in the main two, they are: i) the aerobic pathway, when the chemical reactions include oxygen and ii) the lactic anaerobic pathway, which is mostly used in exhaustive exercise and is characterized by the over production of carbon dioxide and the increase in blood

lactate. In the articles [1] and [2] the concept of anaerobic threshold is introduced. Basically, when the anaerobic threshold is overcome, the anaerobic lactic pathway is activated, which produces ATP through anaerobic glycolysis, to supply the energy requirements of exercise with insufficient oxygen.

In the case of cycling, the power at pedal level gives us a measurement of the mechanical work performed by the cyclist. It is equal to the product of pedaling frequency and torque exerted on the pedal. On the other hand, oxygen consumption and carbon dioxide production provide information about chemical reactions within the body ensuring power production.

In the previous work [6] a gas exchange dynamical model was presented. A version of this model with added state and output disturbances can be written as follows:

$$\mathbf{x}_{k+1} = \mathbf{A}\mathbf{x}_k + \mathbf{B}u_k + \mathbf{B}w_0 + \mathbf{F}d_k \quad (1)$$

$$\mathbf{y}_k = \mathbf{C}\mathbf{x}_k + \mathbf{G}v_k \quad (2)$$

where $\mathbf{x}_k \in \mathbb{R}^3$ is the state vector given by $\mathbf{x}_k = [x_1, x_2, x_3]^T$ with x_1 the consumed oxygen mass per unit time (in g/min), x_2 the mass of carbon dioxide produced aerobically per unit time (in g/min) and x_3 the mass of carbon dioxide produced anaerobically per unit time (in g/min) or excess of CO_2 . The input $u_k \in \mathbb{R}$ stands for the mechanical power at pedal level (in Watts). The symbol w_0 models an additional power consumption required by other physiological tasks that require oxygen consumption and carbon dioxide production. Remark that, at rest $u_k = 0$ and the input w_0 is the only responsible of O_2 consumption and CO_2 production. In this sense the input w_0 corresponds to a constant value, equivalent to the power (in Watts) that produces the basal values of O_2 and CO_2 during rest.

The output vector is defined as $\mathbf{y}_k = [y_1, y_2]^T$ with y_1 the oxygen consumption O_2 and y_2 for the total carbon dioxide production, which is the sum of aerobically produced CO_2 and a fraction of the excess of CO_2 .

The signals d_k and v_k are unknown but bounded disturbances. The products $\mathbf{F}d_k$ and $\mathbf{G}v_k$, with $\mathbf{F} \in \mathbb{R}^3$ and $\mathbf{G} \in \mathbb{R}^2$, model respectively the state and output disturbances.

The system matrices are defined as follows:

$$\mathbf{A} = \begin{bmatrix} \theta_1 & \theta_2 & 0 \\ 0 & \theta_3 & 0 \\ 0 & \theta_5 & \theta_6 \end{bmatrix} \quad \mathbf{B} = \begin{bmatrix} \theta_4 \\ \theta_4 \\ \theta_7 \end{bmatrix} \quad (3)$$

The output matrix is defined as follows:

$$\mathbf{C}(\rho_k) = \begin{bmatrix} 1 & 0 & 0 \\ 0 & 1 & \rho_k \end{bmatrix} \quad (4)$$

Remark that \mathbf{C} depends on a time-varying parameter ρ_k . This varying parameter changes according to the intensity of the exercise.

For the system identification process, two kinds of exercises were performed: i) a sub-maximal exercise or aerobic, where the value of ρ_k is assumed as zero and therefore no

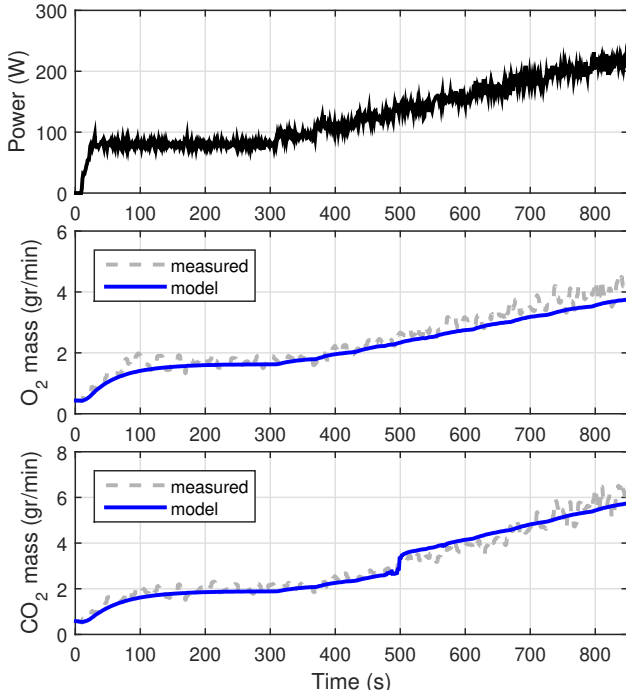


Fig. 2. Obtained FIT of the gas exchange dynamical model with respect to the measured data for an Incremental Cycling Test (ICT).

overproduction of carbon dioxide is considered; ii) a supra-maximal exercise or anaerobic, performed over the anaerobic threshold. In the second case, the value of ρ_k is set to 1 and hence the third state x_3 , i.e. the excess of carbon dioxide is added to the output.

The function hyperbolic tangent, allows us a smooth transition for intermediate values of ρ_k between 0 and 1, which constitutes a third case. To sum up, the values of ρ_k can be written:

$$\rho(z_k) = \begin{cases} 0 & \text{for case 1 : mostly aerobic} \\ 1 & \text{for case 2 : mostly anaerobic} \\ 0.5 + 0.5 \tanh\left(\frac{z_t - z_k}{h}\right) & \text{for case 3 : mixed} \end{cases} \quad (5)$$

The index z_k can be written in terms of the the volume per unit of time of oxygen $\dot{V}O_2$ and the volume per unit of time of carbon dioxide $\dot{V}CO_2$, as follows :

$$z_k = \delta_{O_2} \dot{V}O_{2(k)} - \delta_{CO_2} \dot{V}CO_{2(k)} \quad (6)$$

where the constants δ_{O_2} and δ_{CO_2} correspond to the volumetric mass density in g/l (or equivalently kg/m^3) of O_2 and CO_2 , respectively. The values of z_t and h are parameters calibrated during the identification process proposed in [6].

The outputs of the gas exchange model and measured data of oxygen consumption and carbon dioxide production during an Incremental Cycling Test (ICT) are depicted in Fig. 2. The abrupt change in slope at $t = 500s$ in the plot

of CO_2 mass corresponds to a transition between mostly aerobic (case 1) and mostly anaerobic (case 2) in equation (5), i.e. a change in ρ from 0 to 1.

IV. DESIGN OF A SET-MEMBERSHIP OBSERVER

In order to estimate the quantity of carbon-dioxide production during cycling, the discrete-time system (1) is considered. However, it is assumed the availability of the oxygen consumption measurement only, i.e.:

$$\mathbf{C}(\rho_k) = [1 \ 0 \ 0] \quad (7)$$

In this work, the design of the SMO is performed as proposed in [7]:

$$\hat{\mathbf{x}}_{k+1} = (\mathbf{A} - \mathbf{LC})\mathbf{x}_k + \mathbf{B}u_k + \mathbf{B}w_0 + \mathbf{L}y_k \quad (8)$$

$$\mu_{k+1} = (1 - \lambda)\mu_k + \lambda \quad (9)$$

$$\bar{\mathbf{x}}_k = \hat{\mathbf{x}}_k + \bar{\mathbf{e}}_\infty \mu_k^{1/2} \quad (10)$$

$$\underline{\mathbf{x}}_k = \hat{\mathbf{x}}_k - \bar{\mathbf{e}}_\infty \mu_k^{1/2} \quad (11)$$

where (8) is a punctual observer with a matrix \mathbf{L} computed by using a suitable observer design method based on Linear Matrix Inequalities (LMI). These LMI can be solved by using for instance the CVX solver [13], [14]

Here, the observer gain \mathbf{L} is computed using an H_∞ observer design approach in order to minimize the norm-2 of the estimation error with respect to the norm-2 of the disturbance. Equations (9)-(11) concern the bounds of the state estimation error. These bounds depend on the *a priori* known bounds of the system disturbances. In particular, as it is proposed in [8], the term $\bar{\mathbf{e}}_\infty$, in (10)-(11), stands for a constant column vector defined as follows:

$$\bar{\mathbf{e}}_\infty = \text{diag} \left(\left(\left(\frac{\mathbf{P}}{\lambda \gamma^2 \bar{\mathbf{w}}^T \bar{\mathbf{w}}} \right)^{-1/2} \right) \right) \quad (12)$$

where \mathbf{P} is a positive definite matrix, γ and $\lambda \leq 1$ are positive scalars. Here, the system disturbances $\mathbf{w}_k \in \mathbb{R}^m$ are defined as follows:

$$\mathbf{w}_k := [\mathbf{d}_k \ \mathbf{v}_k]^T \quad (13)$$

The symbol $\bar{\mathbf{w}}$ stands for a vector with positive elements bounding the system disturbances. That is, at every time-instant k , the disturbance satisfies :

$$\mathbf{w}_k^T \mathbf{w}_k \leq \bar{\mathbf{w}}^T \bar{\mathbf{w}} \quad (14)$$

For a given observer gain matrix \mathbf{L} , the matrix \mathbf{P} and the positive scalars γ and λ are obtained by considering the estimation error dynamics:

$$\mathbf{e}_{k+1} = \mathbf{A}_o \mathbf{e}_k + \mathbf{E} \mathbf{w}_k \quad (15)$$

with $\mathbf{A}_o := (\mathbf{A} - \mathbf{LC})$ and $\mathbf{E} := [\mathbf{F} \ -\mathbf{LG}]$. Then, a suitable gain \mathbf{L} stabilizing the dynamics (15) is computed using the Bounded Real Lemma [7]:

Proposition 4.1: (Bounded-real lemma) System (15) is stable if there exist a symmetric positive definite matrix $\mathbf{P} \succ 0$ and a positive scalar $\gamma > 0$ such that,

$$\begin{pmatrix} \mathbf{A}_o^T \mathbf{P} \mathbf{A}_o - \mathbf{P} + \mathbf{Q} & \mathbf{A}_o^T \mathbf{P} \mathbf{E} \\ \mathbf{E}^T \mathbf{P} \mathbf{A}_o & \mathbf{E}^T \mathbf{P} \mathbf{E} - \gamma^2 \mathbf{I}_m \end{pmatrix} \preceq 0 \quad (16)$$

where $\mathbf{Q} \in \mathbb{R}^{n \times n}$ is a given (arbitrary) symmetric positive definite matrix and $\mathbf{I}_m \in \mathbb{R}^{m \times m}$ is an identity matrix. In addition, system (15), with output $\zeta_k := \mathbf{Q}^{1/2} \mathbf{e}_k$ and input \mathbf{w}_k , has a *Quadratic H_∞ performance* equal to γ .

Here, the matrix \mathbf{Q} in (16) is computed as $\mathbf{Q} = \mathbf{V}^{-1}$, where the matrix \mathbf{V} denotes the steady-state estimation error covariance matrix, that can be obtained by solving the following Lyapunov equation, see for instance [15]:

$$\mathbf{A}_o \mathbf{V} \mathbf{A}_o^T - \mathbf{V} = -\mathbf{E} \mathbf{W} \mathbf{E}^T \quad (17)$$

where $\mathbf{W} \in \mathbb{R}^{m \times m}$ concerns the covariance matrix of disturbances \mathbf{w}_k .

Once the matrix \mathbf{P} is obtained for a given matrix \mathbf{Q} , the scalar λ (used in (9) and (12)) is obtained as the minimum generalized eigenvalue of the pair (\mathbf{Q}, \mathbf{P}) .

Finally, in order to initialize the SMO (8)-(11), we suppose that the initial estimation error \mathbf{e}_0 is known and belongs, for instance, to a known ball, that is, $\mathbf{e}_0^T \mathbf{e}_0 \leq \delta^2$, for a given constant positive scalar δ . Then, as stated in [7], the initial value of the scalar μ in (9) has to verify:

$$\mu_0 \geq \lambda_{max}(\mathbf{P}) \delta^2 / \bar{c} \quad (18)$$

with $\bar{c} = \frac{1}{\lambda} \gamma^2 \bar{\mathbf{w}}^T \bar{\mathbf{w}}$.

The complete observer design process is summarizing in Algorithm 1.

Algorithm 1 Set-membership observer design.

Require: Matrices $\mathbf{A}, \mathbf{B}, \mathbf{C}, \mathbf{F}$ and \mathbf{G} describing system (1), the observer gain \mathbf{L} obtained by performing an H_∞ observer synthesis and the covariance matrix of disturbances \mathbf{W} .

- 1: Compute $\mathbf{A}_o = \mathbf{A} - \mathbf{L}\mathbf{C}$.
 - 2: Compute $\mathbf{E} = [\mathbf{F} \quad -\mathbf{L}\mathbf{G}]$
 - 3: Compute the covariance matrix \mathbf{V} using (17).
 - 4: Do $\mathbf{Q} = \mathbf{V}^{-1}$.
 - 5: Find a matrix \mathbf{P} and the minimum γ who satisfy the LMI (16).
 - 6: Compute λ as the minimum generalized eigenvalue of the pair (\mathbf{Q}, \mathbf{P}) .
 - 7: **return** The observer parameters $\mathbf{L}, \mathbf{P}, \gamma$ and λ .
-

V. EXPERIMENTAL VALIDATION

A. System identification

Experimental data was obtained using a Hammer Trainer for measurements of power and cadence, a Metalyzer 3B Cortex for measurements of the oxygen consumption and carbon dioxide production and a bluetooth sensor Polar



Fig. 3. Experimental setup for cycling tests: system identification and state observer validation.

H10 for measurements of the heart rate. Gas exchange data was collected breath-by-breath and then resampled by interpolation with a constant sampling period of 1 second. The Fig. 3 shows the subject of study performing one of the cycling tests.

The methodology described in [6] is followed to compute the matrices of the system :

$$\mathbf{A} = \begin{bmatrix} 0.944 & 0.029 & 0 \\ 0 & 0.981 & 0 \\ 0 & 0.001 & 0.994 \end{bmatrix} \quad \mathbf{B} = \begin{bmatrix} 0.363 \\ 0.363 \\ 0.023 \end{bmatrix} \times 10^{-3} \quad (19)$$

and the parameters $w_0 = 18.288$, $\mathbf{z}_t = -0.507$ and $h = 0.0452$.

The parameters of the system are chosen to fit the behaviour of a single individual, however the model structure does not change for different individuals.

B. Estimation of the disturbances bounds

Section IV describes that the system is affected by unknown and bounded state and output disturbances. This section describes a method for estimating the bounds of the disturbances.

The output error or measurement error in (2), denoted now as $\mathbf{G}v_k$, can be estimated thanks to the availability of measured data. This error is used for the identification and further validation of the model.

The output error $\tilde{\mathbf{y}}$, called also the residual, is defined as the difference between the model output \mathbf{y}_k^I and the measured data. Since the measurements correspond to O_2 and CO_2 flows and the model outputs are in mass units, it is necessary to calculate the equivalent masses using the density of the gases. With the equivalent of the measurements in mass, \mathbf{y}_k^D , the residual equation is :

$$\tilde{\mathbf{y}}_k = \mathbf{y}_k^I - \mathbf{y}_k^D \quad (20)$$

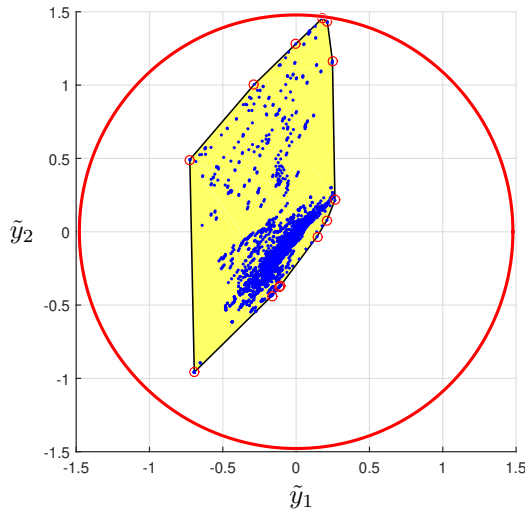


Fig. 4. Ball containing all the output errors from the identified system.

The model identification was performed using measurements of the mass of oxygen consumption (y_1) and of the mass of total carbon dioxide production (y_2), i.e. the vector $\mathbf{y} = [y_1, y_2]^T$.

The values of the obtained residuals can be depicted in an output error space $(\tilde{y}_1, \tilde{y}_2)$ as it is shown in Fig. 4.

From this figure, a polyhedron which contains all the output error points can be calculated. After that, a ball which contains the furthest vertex of the polyhedron can be also calculated, and then, the radius of that ball is considered to be a bound of the output disturbances. Here we have a radius equal to 1.478.

As it can be seen in Fig. 4, the ball is a conservative estimation of the error, but ensures the inclusion of all possible measurement errors. Thus for the output given by (2) which is considered as the only output for the SMO, we set $G_1 = 1.478$ and $|v_k| \leq 1$.

Concerning process disturbances and/or model errors, we assume the existence of additive disturbances with maximum amplitudes corresponding to 30% of the constant input $\mathbf{B}w_0$. That is, the bounds of those disturbances will be equal to 1.993×10^{-3} affecting every system state. In particular, it is chosen process disturbances modeled by a column vector $\mathbf{F} = 1.993 \times 10^{-3}[1, 1, 1]^T$ and an input $|d_k| \leq 1$. In this way all the disturbances (process and measurement disturbances) have been normalized by suitable scaling their input matrices.

C. Computation of observer gain matrix

A SMO is designed by using Algorithm 1. The obtained observer gain is $\mathbf{L} = [0.157 \ 0.064 \ 0.012]^T \times 10^{-3}$.

The disturbance covariance matrix is chosen to be $\mathbf{W} = \text{diag}([0.33, 0.33])$, which suppose that the normalized disturbances v_k and d_k are bounded disturbances with uniform

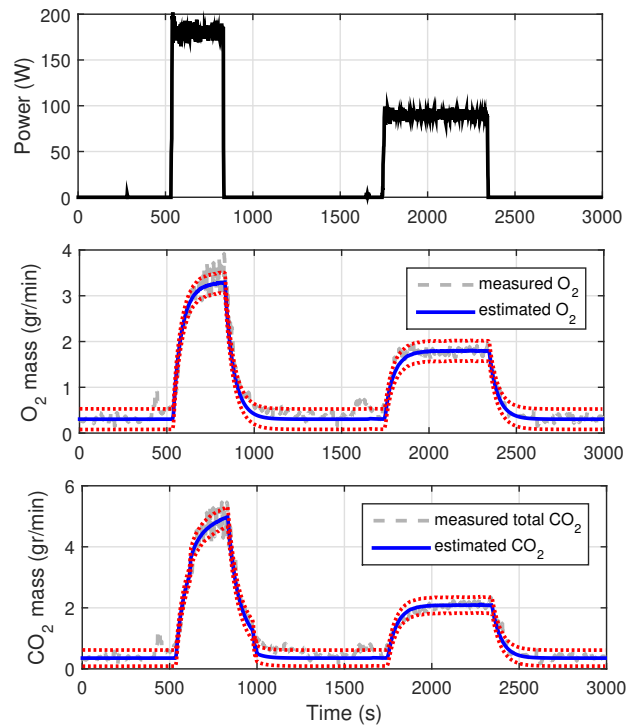


Fig. 5. Results of the set-membership observer Grey signals are measured, blue signals are the estimated signals and red dotted signals are the estimation error bounds.

probability distribution. Thus, the obtained matrix \mathbf{Q} is :

$$\mathbf{Q} = \begin{bmatrix} 6.37 & -5.93 & 1.63 \\ -5.93 & 5.58 & -1.73 \\ 1.63 & -1.73 & 2.01 \end{bmatrix} \times 10^6 \quad (21)$$

After solving the LMI given by (16) using (21), the matrix \mathbf{P} and the minimum value of γ are :

$$\mathbf{P} = \begin{bmatrix} 2.26 & -2.00 & 0.22 \\ -2.00 & 1.92 & -0.54 \\ 0.22 & -0.54 & 2.97 \end{bmatrix} \times 10^8 \quad \gamma = 37.96 \quad (22)$$

Finally, the scalar λ was 2.612×10^{-3} , computed as the minimum generalized eigenvalue of the pair (\mathbf{Q}, \mathbf{P}) .

Using all the previous observer parameters and equation (12), the following element-wise steady-state estimation-error bounds was computed $\bar{\mathbf{e}}_\infty = [0.222 \ 0.262 \ 0.063]^T$.

The observer validation is performed with an initial value of μ_0 (used in (9)) equal to 2, which means that the initial value of the estimation error vector is twice the amplitude of the estimation error vector at steady-state value. This assumption ensures the inclusion of initial conditions and therefore verifies (18).

D. Simulation results of state estimation

The results of the estimation of carbon dioxide production are shown in Fig. 5. In addition, the measured data is included for comparison. This scenario contains two different

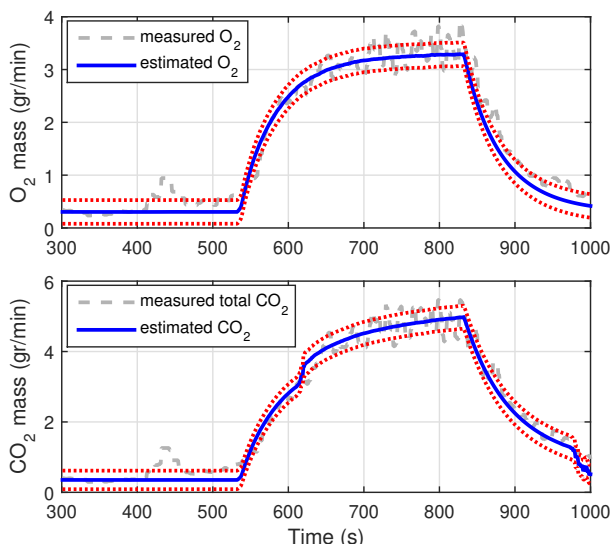


Fig. 6. Zoom of the outputs of Fig. 5 between $t=300$ s and 1000 s. Data outside the bounds are noise with respect the dynamical model.

intensities of exercise: a high intensity exercise followed by a moderate intensity exercise.

The dotted lines correspond to the state bounds obtained from the set-membership state observer. Remark that carbon dioxide production (CO_2 mass) concerns the sum of two system states, then its error bounds will result from the operation of the bounds of both states.

Some trajectories in Fig. 6 are measurements outside of the predetermined bounds, for instance between $t = 400$ s and 500s, when movements of the cyclist and gas exchange variables are not related with pedal power. A similar situation occurs during high levels of exercise (between $t=700$ s and 800s), where hyperventilation occurs. These phenomena are related to state trajectories that are not depending on the pedal power, and it is thus normal that the proposed observer bounds do not include those trajectories. In addition, by assumption we consider bounded disturbances whose values of the bounds are obtained from the identification process. Even if this assumption is not realistic for unbounded stochastic disturbances, the proposed approach could be useful for determining a level of the estimation uncertainty for a given possible amplitude of disturbances.

VI. CONCLUSIONS AND PERSPECTIVES

In this paper, we presented a design method to compute the gain of a robust set-membership state observer as well as deterministic bounds for the estimation error for a disturbed linear system.

The methodology is applied to a model of gas exchange dynamics in order to estimate gas exchange during cycling, based on a measure of power at the pedal and oxygen consumption. To do so, the disturbances affecting the gas exchange system are quantified by analyzing the distribution of the output error of the model in the residual space. The performances of the aforementioned state observer are

assessed in simulation using experimental data. The gas exchange variables are successfully estimated along the cycling test and the bounds for the estimation error properly framed the experimental signals.

The obtained results motivate its use for gas exchange estimation for which the number of sensors has to be reduced, especially for embedded applications.

REFERENCES

- [1] K. Wasserman, B. J. Whipp, S. Kooyl, and W. Beaver, "Anaerobic threshold and respiratory gas exchange during exercise.," *Journal of applied physiology*, vol. 35, no. 2, pp. 236–243, 1973.
- [2] W. L. Beaver, K. Wasserman, and B. J. Whipp, "A new method for detecting anaerobic threshold by gas exchange.," *Journal of applied physiology*, vol. 60, no. 6, pp. 2020–2027, 1986.
- [3] T. Leitner, H. Kirchsteiger, H. Trogmann, and L. del Re, "Model based control of human heart rate on a bicycle ergometer," in *European Control Conference (ECC)*, 2014, pp. 1516–1521, IEEE, 2014.
- [4] D. Meyer, W. Zhang, and M. Tomizuka, "Sliding mode control for heart rate regulation of electric bicycle riders," in *ASME 2015 Dynamic Systems and Control Conference*, pp. V002T27A003–V002T27A003, American Society of Mechanical Engineers, 2015.
- [5] M. Corno, P. Giani, M. Tanelli, and S. M. Savaresi, "Human-in-the-loop bicycle control via active heart rate regulation," *Control Systems Technology, IEEE Transactions on*, vol. 23, no. 3, pp. 1029–1040, 2015.
- [6] N. Rosero, J. J. Martinez, and M. Corno, "Modeling of gas exchange dynamics using cycle-ergometer tests," in *Proceedings of 9th Mathmod conference*, vol. 24, pp. 1247–1256, Vienna, 2018.
- [7] N. Loukkas, J. J. Martinez, and N. Meslem, "Set-membership observer design based on ellipsoidal invariant sets," in *Proceedings of the IFAC World Congress*, 2017.
- [8] J. Martinez, N. Loukkas, and N. Meslem, "H-infinity set-membership observer design for discrete-time lpv systems," *International Journal of Control*, vol. 93, no. 10, pp. 2314–2325, 2020.
- [9] D. J. Macfarlane, "Automated Metabolic Gas Analysis Systems: A Review," *Sports Medicine*, vol. 31, no. 12, pp. 841–861, 2001.
- [10] G. Atkinson, R. C. R. Davison, and A. M. Nevill, "Performance Characteristics of Gas Analysis Systems: What We Know and What We Need to Know," *International Journal of Sports Medicine*, vol. 26, pp. S2–S10, Feb. 2005.
- [11] J. J. Ramos-Álvarez, I. Lorenzo-Capellá, and F. J. Calderón-Montero, "Disadvantages of Automated Respiratory Gas Exchange Analyzers," *Frontiers in Physiology*, vol. 11, p. 19, Feb. 2020.
- [12] M. Folke, L. Cernerud, M. Ekström, and B. Hök, "Critical review of non-invasive respiratory monitoring in medical care," *Medical & Biological Engineering & Computing*, vol. 41, pp. 377–383, July 2003.
- [13] M. Grant and S. Boyd, "CVX: Matlab software for disciplined convex programming, version 2.1." <http://cvxr.com/cvx>, Mar. 2014.
- [14] M. Grant and S. Boyd, "Graph implementations for nonsmooth convex programs," in *Recent Advances in Learning and Control* (V. Blondel, S. Boyd, and H. Kimura, eds.), Lecture Notes in Control and Information Sciences, pp. 95–110, Springer-Verlag Limited, 2008. http://stanford.edu/~boyd/graph_dcp.html.
- [15] E. Kofman, J. De Dona, and M. M. Seron, "Probabilistic set invariance and ultimate boundedness," *Automatica*, vol. 48, no. 10, pp. 2670 – 2676, 2012.